Bioscience Reports

www.bioscirep.org

G-protein coupled receptor solubilization and purification for biophysical analysis and functional studies, in the total absence of detergent

Mohammed Jamshad*[1], Jack Charlton*[1], Yu-Pin Lin*[1], Sarah J. Routledge†[1], Zharain Bawa†, Timothy J. Knowles‡, Michael Overduin‡, Niek Dekker§, Tim R. Dafforn*, Roslyn M. Bill†, David R. Poyner† and Mark Wheatley*[2]

*School of Biosciences, University of Birmingham, Edgbaston, Birmingham, B15 2TT, U.K.
†School of Life and Health Sciences, Aston University, Birmingham B4 7ET, U.K.
‡School of Cancer Studies, University of Birmingham, Edgbaston, Birmingham, B15 2TT, U.K.
§Discovery Sciences, AstraZeneca R&D Mölndal, 43183 Mölndal, Sweden.

Synopsis

G-protein coupled receptors (GPCRs) constitute the largest class of membrane proteins and are a major drug target. A serious obstacle to studying GPCR structure/function characteristics is the requirement to extract the receptors from their native environment in the plasma membrane, coupled with the inherent instability of GPCRs in the detergents required for their solubilization. In the present study, we report the first solubilization and purification of a functional GPCR [human adenosine A_{2A} receptor ($A_{2A}R$)], in the total absence of detergent at any stage, by exploiting spontaneous encapsulation by styrene maleic acid (SMA) co-polymer direct from the membrane into a nanoscale SMA lipid particle (SMALP). Furthermore, the $A_{2A}R$–SMALP, generated from yeast (*Pichia pastoris*) or mammalian cells, exhibited increased thermostability ($\sim 5\,°C$) compared with detergent [DDM (n-dodecyl-β-D-maltopyranoside)]-solubilized $A_{2A}R$ controls. The $A_{2A}R$–SMALP was also stable when stored for prolonged periods at $4\,°C$ and was resistant to multiple freeze-thaw cycles, in marked contrast with the detergent-solubilized receptor. These properties establish the potential for using GPCR–SMALP in receptor-based drug discovery assays. Moreover, in contrast with nanodiscs stabilized by scaffold proteins, the non-proteinaceous nature of the SMA polymer allowed unobscured biophysical characterization of the embedded receptor. Consequently, CD spectroscopy was used to relate changes in secondary structure to loss of ligand binding ([^{3}H]ZM241385) capability. SMALP-solubilization of GPCRs, retaining the annular lipid environment, will enable a wide range of therapeutic targets to be prepared in native-like state to aid drug discovery and understanding of GPCR molecular mechanisms.

Key words: adenosine receptor, detergent-free, G-protein coupled receptor (GPCR), protein thermostability, structure.

INTRODUCTION

G-protein coupled receptors (GPCRs) constitute the largest class of membrane proteins in the human genome with >800 unique receptors. They are activated by an extremely diverse range of stimuli which differ with respect to their physico-chemical properties and size; ranging from photons, through small biogenic amines to peptides and glycoproteins [1]. GPCRs share a common protein architecture comprising seven transmembrane helices and are represented in the genome of organisms from viruses and slime moulds to plants and humans. Consequently, these receptors are central to cell signalling and as such are important to the pharmaceutical industry as therapeutic targets in drug discovery

programs. Indeed, 40%–50% of clinically-prescribed drugs and ~25% of the top selling drugs target this protein family [2].

A pre-requisite to a detailed understanding of the molecular mechanisms underlying ligand binding, receptor activation and intracellular signalling is the ability to study the receptor protein in isolation while preserving the GPCR protein-fold and pharmacology. Extracting GPCRs from the cell membrane to produce a solubilized preparation for studying receptor structure and function has universally involved the use of a class of surfactants often referred to as detergents. These detergents not only disrupt the cell membrane but also simultaneously substitute for the native lipid in close association with the membrane protein (annular lipid). Unfortunately, inserting a protein into a detergent micelle provides only a poor approximation of the cell membrane bilayer and the native annular lipid. Indeed, it is thought that delipidation may be the most common cause of membrane protein inactivation during solubilization [3]. Once solubilized by a detergent, all subsequent studies require the continued presence of detergent to prevent receptor aggregation, despite the problems this causes with respect to receptor stability. This inherent instability of GPCRs in detergent micelles was the motivation for the development a new class of detergent, maltose-neopentyl glycol amphiphiles, designed specifically to improve GPCR stability during solubilization and crystallization studies [4]. An alternative strategy is to exchange the detergent used to solubilize GPCRs [often n-dodecyl-β-D-maltopyranoside (DDM)] with a non-conventional surfactant, such as amphipathic polymers (amphipols) or fluorinated surfactants [5,6]. The use of these non-conventional surfactants does not obviate the use of classical detergents however, as amphipols and fluorinated surfactants are usually incapable of solubilizing proteins directly from the plasma membrane [3]. Using an alternative strategy, an engineered β-sheet peptide was used to stabilize detergent-solubilized membrane proteins, including the glucagon receptor [7]. Another approach, pioneered by the Sligar laboratory [8] and subsequently utilized by other groups, is to encapsulate detergent-solubilized receptors into nanodiscs [9–11]. Nanodiscs are nanometre-scale planar discs of lipid bilayer stabilized by encircling membrane scaffold protein (MSP), usually a modified form of human high-density lipoprotein apoA-1 [12,13]. This encapsulation of GPCRs into nanodiscs is usually performed using receptor that was previously purified in detergent. However, the parathyroid hormone 1 receptor (PTH1R) was recently purified in nanodiscs following initial solubilization by the detergent DDM, specifically to reduce the time the PTH1R was exposed to detergent [14]. Nevertheless, a general limitation of nanodiscs is that interference from the obligatory stabilizing scaffolding protein prevents or perturbs the downstream application of many biophysical approaches to study the encapsulated protein of interest.

There has been an absolute requirement for detergent to solubilize GPCRs despite the universal acknowledgement that exposing GPCRs to detergent perturbs and destabilizes the receptor. Although significant progress has been made to reduce the detrimental impact of detergent by employing non-conventional surfactants or nanodiscs, the ideal situation would be to generate GPCRs in aqueous solution in a native-like state, complete with annular lipid, but without any exposure to detergent. In the present study, we report the first solubilization and purification of a GPCR, the human adenosine A_{2A} receptor (A_{2A}R), without the use of detergent at any stage by exploiting spontaneous encapsulation of a GPCR direct from a membrane into a nanoscale styrene maleic acid (SMA) lipid particle (SMALP). This generates a nano-section of the native membrane excised and stabilized by a ring of SMA polymer [15]. In addition, we demonstrate the utility of our approach by applying SMALP-solubilization to two applications fundamentally important to GPCR research: (i) purification of milligram amounts of functional GPCR from a commonly employed overexpression system (yeast) and (ii) solubilization of GPCR from transfected mammalian cells in culture, with retention of the annular native membrane environment, for downstream applications, such as drug discovery assays.

EXPERIMENTAL

Materials

[^{3}H]ZM241385 (specific activity 50.0 Ci/mmol) was purchased from American Radiolabelled Chemicals. ZM241385 {4-(2-[7-amino-2-(2-furyl)[1,2,4]triazolo[2,3-a][1,3,5]triazin-5-yl amino]ethyl)phenol} was purchased from Tocris, xanthine analogue congener (XAC), 5'-(N-ethylcarboxamido)adenosine (NECA) and theophylline from Sigma. Cell culture media, buffers and supplements were purchased from Invitrogen. Restriction enzymes were obtained from NEB.

Expression of A_{2A}R in *P. pastoris*

General protocols for heterologous expression of A_{2A}R in *P. pastoris* were as described in the *Pichia* Fermentation Process Guidelines (Invitrogen) or as described previously [16,17]. The human A_{2A}R was expressed with an N-terminal His$_{10}$-tag in the pPICZαA expression plasmid and incorporated an Asn154Gln mutation to preclude hyperglycosylation [18]. The A_{2A}R–pPICZαA expression plasmid was linearized, purified and used to transform *P. pastoris strain* X-33 by electroporation. Colonies were selected on yeast extract peptone dextrose sorbitol plates containing 0.1 mg/ml Zeocin and then used for receptor expression screening. Small-scale screening and protein detection was carried out as described previously [16] with the following modifications; the induction temperature was lowered to 22°C and the A_{2A}R antagonist theophylline (10 mM) was added at the point of induction [18]. For large-scale expression of A_{2A}R, frozen glycerol stock culture was used to inoculate 50 ml of buffered complex glycerol medium (1% yeast extract, 2% peptone, 1.34% yeast nitrogen base without amino acids, 0.00004% biotin, 1% glycerol, 0.1 M phosphate buffer, pH 6) containing 100 μg/ml Zeocin. The cells were grown at 30°C and 220 rpm overnight to yield an optical density at 600 nm (D_{600}) of 2–6. A 50 ml aliquot of this culture was used to inoculate a 1 l of fermenter (Applikon) containing basal salts medium (BSM)

plus *Pichia* trace minerals 1 (PTM$_1$) trace salts to a starting D_{600} of 0.3. The fermentation run in 'fed-batch' mode at 30°C and pH 5.0 was maintained using undiluted (28%) ammonium hydroxide. Dissolved oxygen (DO) was maintained above 20% saturation by adjusting agitation rate and pure oxygen supply.

When the initial glycerol (40 g/l) in batch phase was depleted, as indicated by a spike in DO reading, a 50% (w/v) glycerol solution containing 1.2% (v/v) PTM$_1$ was introduced at a feed rate of 30 ml/h for 4 h. Glycerol feed was terminated followed by a 3 h starvation phase to achieve complete glycerol consumption. During the final hour of starvation, the temperature was reduced from 30°C to 22°C and allowed to stabilize. Theophylline (10 mM) was then added to the culture to increase A$_{2A}$R stabilization during expression. The cells were induced with 100% methanol containing 1.2% (v/v) PTM$_1$ at an initial feed rate of 1.92 ml/h for 17 h to allow culture adaptation to methanol. When a steady DO rate and fast DO spike time was obtained, indicative of adaptation to methanol utilization, the feed rate was increased to 3.96 ml/h for the remainder of the fermentation. The entire methanol 'fed-batch' phase lasted approximately 40 h with a total of ~125 ml of methanol fed per litre of initial volume. The cells were then harvested by centrifugation at 6000 *g* in a Beckman JLA-8.1 rotor and washed once with 10 mM Tris/HCl buffer, pH 8.

Yeast Membrane preparation

Yeast cells expressing A$_{2A}$R were disrupted as described previously [16]. The membranes were resuspended to 80 mg/ml in 50 mM Tris/HCl, 10% glycerol, 500 mM NaCl, pH 8 and used immediately for SMA solubilization or snap-frozen and stored at −80°C until further use.

HEK293T cell culture and transfection

Human embryonic kidney (HEK)293T cells were routinely cultured in Dulbecco's modified Eagles medium (DMEM) containing L-glutamine (2 mM), D-glucose (4500 mg/l) and sodium pyruvate (1mM) supplemented with 10% (v/v) fetal calf serum (FCS) in humidified 5% (v/v) CO$_2$ in air at 37°C. Transfection was essentially as described previously [19]. Cells were seeded at a density of ~5 × 10^5 cells/100-mm dish and transfected after 48 h using a mixture of 5 μg of DNA, 60 μl of polyethyleneimine (10 mM) and 1 ml of 5% glucose solution, which was incubated for 30 min at room temperature before addition to an appropriate final volume of full media. A$_{2A}$R-expressing HEK293T cells were used 48 h post-transfection.

Preparation of styrene maleic acid co-polymer

Poly(styrene-co-maleic anhydride) with a ratio of 2:1 styrene to maleic anhydride was used as described in [15]. Briefly, a 10% solution of SMA co-polymer in NaOH (1 M) was refluxed for 2 h and allowed to cool to room temperature, then dialysed against buffer before use.

SMA solubilization of A$_{2A}$R

A$_{2A}$R-expressing yeast membranes, at a final concentration of 40 mg/ml (wet weight) were incubated with SMA (2.5% w/v final concentration) for 20 h at 25°C with gentle stirring. Non-solubilized material was sedimented at 100 000 *g* for 1 h at 4°C, to yield a supernatant containing A$_{2A}$R–SMALP. HEK293T cells transiently transfected with A$_{2A}$R were washed with ice-cold PBS 48 h post-transfection, then scraped into 1 ml/dish of harvesting buffer (20 mM HEPES, 1 mM EGTA, 1 mM magnesium acetate, pH 7.4) containing 2% (w/v) SMA and 5 units/ml of benzonase. Samples were incubated at 37°C for 1 h before centrifugation at 100 000 *g* for 1 h at 4°C.

DDM solubilization of A$_{2A}$R

Yeast membranes containing A$_{2A}$R were solubilized with DDM in solubilization buffer [50 mM Tris/HCl, 10% glycerol, 500 mM NaCl, 2.5% (w/v) DDM, 0.5% (w/v) cholesteryl hemi-succinate, plus complete EDTA-free protease inhibitor cocktail (Roche), pH 8.0] with a final concentration of 40 mg/ml (wet weight). After incubation with slow rotation at 4°C for 2 h, the sample was centrifuged at 100 000 *g* for 1 h at 4°C to remove the non-solubilized material. For HEK293T cells, a crude membrane preparation was prepared as described previously [20] and the protein concentration determined using the BCA protein assay kit (Pierce) using BSA as standard. A$_{2A}$R-expressing membranes (final protein concentration 0.5 mg/ml) were incubated with solubilization buffer (20 mM HEPES, 1mM EGTA, 1 mM magnesium acetate, 2.5% (w/v) DDM, 0.5% (w/v) cholesteryl hemi-succinate, plus complete EDTA-free protease inhibitor cocktail (Roche) for 3 h at 4°C.

Ni^{2+}–NTA affinity purification

The SMA-solubilized preparation was recirculated through a HisTrap HP 1 ml Ni^{2+}–NTA (nitrilotriacetate) Sepharose (GE Healthcare) overnight at 4°C. The column was washed with 20 column volumes (cv) of 50 mM Tris/HCl, pH 8.0, 500 mM NaCl, 10% glycerol, 20–60 mM imidazole, complete EDTA-free protease inhibitor. Elution of the A$_{2A}$R–SMALP was achieved using 250 mM imidazole (10 cv) collected in 0.5 ml fractions. Eluted fractions containing A$_{2A}$R–SMALP were pooled, dialysed overnight against buffer (50 mM Tris/HCl, 150 mM NaCl, 10% glycerol, complete protease inhibitor then concentrated using a centrifugal concentrator (Vivaspin 20, 30 kDa cut-off, Sigma)). Western blotting analysis used a primary anti-histidine antibody (Takara Bio Europe) and an anti-mouse-HRP (horseradish peroxidase; NEB) secondary antibody (both at 1:5000 dilution) visualized using a chemiluminescence detection kit (Geneflow).

Radioligand-binding assays

Competition radioligand-binding assays with A$_{2A}$R–SMALP used [^{3}H]ZM241385 (1 nM) as tracer ligand plus competing ligand at the concentrations indicated in a final volume of 250 μl. Non-specific binding was defined by unlabelled ZM241385

(1 μM). After incubation at 30°C for 30 min to establish equilibrium, bound and free ligand were separated by P30 minispin gel filtration columns (1000 g, 4 min). Bound ligand in the void volume was quantified by liquid scintillation counting using a Packard Tri-Carb Liquid Scintillation Counter with HiSafe3 (Perkin–Elmer) as cocktail. Binding data were analysed by non-linear regression to fit theoretical Langmuir binding isotherms (with Hill slopes constrained to unity) to the experimental data using PRISM (Graphpad Software Inc.). K_i values were calculated from IC_{50} values using the Cheng–Prusoff equation to correct for radioligand occupancy [21].

Gel filtration analysis

Gel filtration experiments were performed at 20°C using a Superdex 200 10/300 GL column pre-equilibrated with buffer (50 mM Tris, 300 mM NaCl, pH 8.0) on an ÄKTA Purifier system (GE Healthcare) with a flow rate of 1 ml/min. All experiments were performed using 50 mM Tris, pH 8, with 300 mM NaCl using a flow rate of 1 ml/min. The column was calibrated using the standards ovalbumin (43 kDa), canalbumin (75 kDa), aldolase (158 kDa), ferritin (440 kDa) and thyroglobulin (669 kDa) (GE Healthcare).

CD

Data between 260 and 195 nm were collected using a JASCO J-715 Spectrapolarimeter with a 1 mm path length cuvette containing 0.05 mg/ml protein. Each spectrum was collected with a data pitch of 0.5 nm and represents the average of eight scans. Data were also collected using the same parameters for cuvettes containing the relevant buffer to allow subtraction of the buffer contribution.

Sedimentation velocity analytical ultracentrifugation

Purified $A_{2A}R$–SMALP equilibrated in 10 mM sodium phosphate, pH 8.0, was characterized by analytical ultracentrifugation (AUC). Velocity experiments were performed using a Beckman Coulter XL-I analytical ultracentrifuge (Beckman 693 Coulter) with a Ti50 rotor at 40000 rpm (129 000 g) at 4°C. The protein within the cell was monitored by absorbance at 280 nm. Data were then analysed using the c(S) and c(M) routines implemented within SEDFIT, a sedimentation data-fitting program [22]. Parameters for $A_{2A}R$ vbar and solvent density and viscosity were calculated using SEDNTERP, a sedimentation interpretation program [23].

RESULTS AND DISCUSSION

Detergent-free purification of the $A_{2A}R$ expressed in yeast using SMALPs

The yeast *P. pastoris* has been utilized extensively to overexpress a wide range of membrane proteins from a variety of organisms,

Table 1 Pharmacological characterization of $A_{2A}R$–SMALP from *P. pastoris*
For each ligand, the pK_i value is presented for binding to $A_{2A}R$ expressed in *P. pastoris* membranes and also $A_{2A}R$–SMALP generated from the *P. pastoris* membranes. Data are mean $\pm$ S.E.M. ($n = 3$).
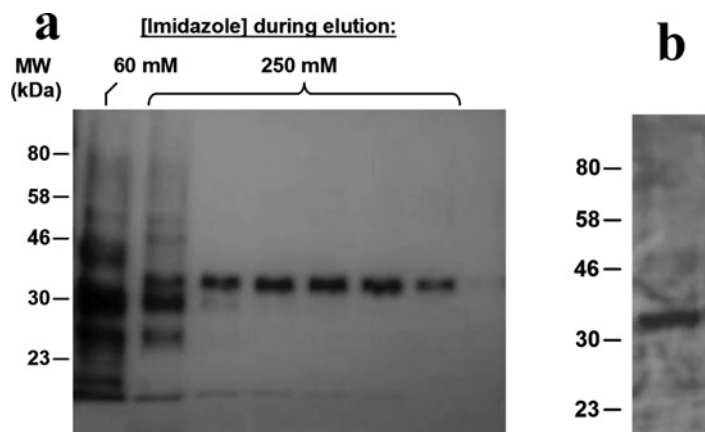
Ligand	Yeast membrane	Yeast-SMALP
ZM241385	7.95 ± 0.45	7.79 ± 0.14
XAC	6.53 ± 0.24	7.16 ± 0.18
NECA	5.66 ± 0.26	5.43 ± 0.1
Theophylline	3.82 ± 0.30	4.13 ± 0.1

including GPCRs for crystallization [24,25]. A histidine-tagged human $A_{2A}R$ was expressed in a genetically-engineered strain of *P. pastoris*, developed specifically for high-level expression of recombinant membrane protein [26], using culture conditions optimized for production of functional receptor. $A_{2A}R$-expressing yeast cells were disrupted [16], then directly solubilized with 2.5 % (w/v) SMA co-polymer in the total absence of detergent. The membrane pellet visibly clarified upon exposure to SMA due to SMALP formation. Following removal of non-solubilized material by centrifugation (100 000 g, 1h), the $A_{2A}R$–SMALP was purified using Ni^{2+}–NTA linked agarose (Figure 1a). The $A_{2A}R$ eluted as a single band in fractions containing 250 mM imidazole. The identity of the band as the $A_{2A}R$ was confirmed by Western blotting using anti-histidine antibody to detect the histidine-tagged $A_{2A}R$ (Figure 1b) and partial sequencing of the purified protein using Fourier-transform ion cyclotron resonance (FTICR) MS. The FTICR identified three peptides YNGLVT-GTR, QMESQPLPGER and SHVLRQQEPFK corresponding to $A_{2A}R$ residues 112–120 (part of intracellular loop 2), 210–220 (part of intracellular loop 3) and 305–315 (part of the C-terminal tail) respectively.

Radioligand-binding assays with [³H]ZM241385 established that the binding (B_{max}) of the purified $A_{2A}R$–SMALP preparation was 20 100 pmol/mg protein, consistent with the theoretical value for fully active receptor (21 300 pmol/mg protein), compared with 9.5 pmol/mg protein in the original yeast membrane. Competition ligand binding assays using a range of ligands with $A_{2A}R$–SMALP were consistent with established $A_{2A}R$ pharmacology (International Union of Pharmacology (IUPHAR) database) and comparable to $A_{2A}R$ binding in the original yeast membranes (Table 1).

Several nanoscale self-assembly reagent systems have been reported for purifying membrane proteins including bicelles, amphipols, scaffolding protein-stabilized nanodiscs and SMALPs [27]. However, of these, only SMALP-solubilization of GPCRs; (i) avoids exposure to detergent at any stage, (ii) preserves the native composition of the annular lipid in close association with the receptor and (iii) retains the lateral pressure exerted within the membrane bilayer that has been shown to be important for maintaining the conformation of membrane proteins [28]. Previous studies have shown that membrane proteins could be SMALP-solubilized from prokaryotes, such as archaea and bacteria [15,29] and also from eukaryotic cells [30], but this is the first report that a GPCR can be SMALP-solubilized and

Figure 1   Purification of SMALP-solubilized His-tagged A$_{2A}$R from *P. pastoris*
(**a**) The A$_{2A}$R eluted from the Ni^{2+}–NTA linked agarose as a single band in silver-stained fractions with 250 mM imidazole.
(**b**) Western blot of the 250 mM imidazole fraction with an anti-histidine antibody.

furthermore that the active receptor can be purified to homogeneity as a GPCR–SMALP without the use of detergent at any stage.
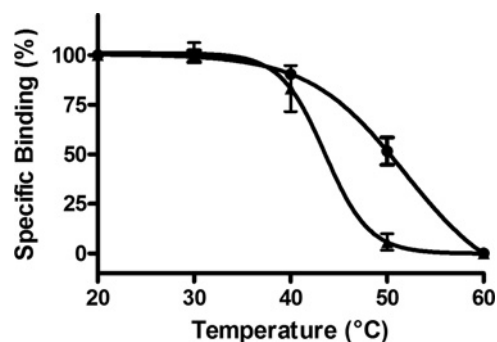
Increased thermostability of A$_{2A}$R–SMALP compared with detergent-solubilized A$_{2A}$R

An acknowledged common problem with detergent solubilization of GPCRs is destabilization of the receptor in the detergent micelle compared with the native plasma membrane. As the A$_{2A}$R–SMALP preserves the annular lipid in close contact with the receptor in the membrane, it was reasoned that A$_{2A}$R would be more thermostable in a SMALP than when detergent-solubilized by DDM, a widely employed detergent for GPCR solubilization. The antagonist [^{3}H]ZM241385 is widely used to quantify functional A$_{2A}$R-binding capability using radioligand-binding assays. A$_{2A}$R–SMALP and DDM-solubilized A$_{2A}$R from *P. pastoris* membranes were incubated in parallel at various temperatures and then the residual specific binding of [^{3}H]ZM241385 was determined. From data presented in Figure 2, it can be seen that the SMALP conferred a marked increase in A$_{2A}$R thermostability of ∼5.5 °C over the detergent micelle, with the T$_{50}$ value increasing from T$_{50}$ = 44.4 ± 0.27 °C (n = 3) for A$_{2A}$R–DDM to T$_{50}$ = 49.9 ± 1.19 °C (n = 3) for A$_{2A}$R–SMALP.

Biophysical characterization of purified A$_{2a}$R–SMALP

Characterization of the A$_{2A}$R–SMALP by size-exclusion chromatography revealed a mono-dispersed particle (Figure 3a). Analysis of the main peak by SDS/PAGE revealed a single protein band (Figure 3b) with a migration consistent with the A$_{2A}$R (compare with Figure 1). AUC of the A$_{2A}$R–SMALP confirmed the presence of a single major particle species with a sedimentation coefficient of 2.3S (Figure 3c).
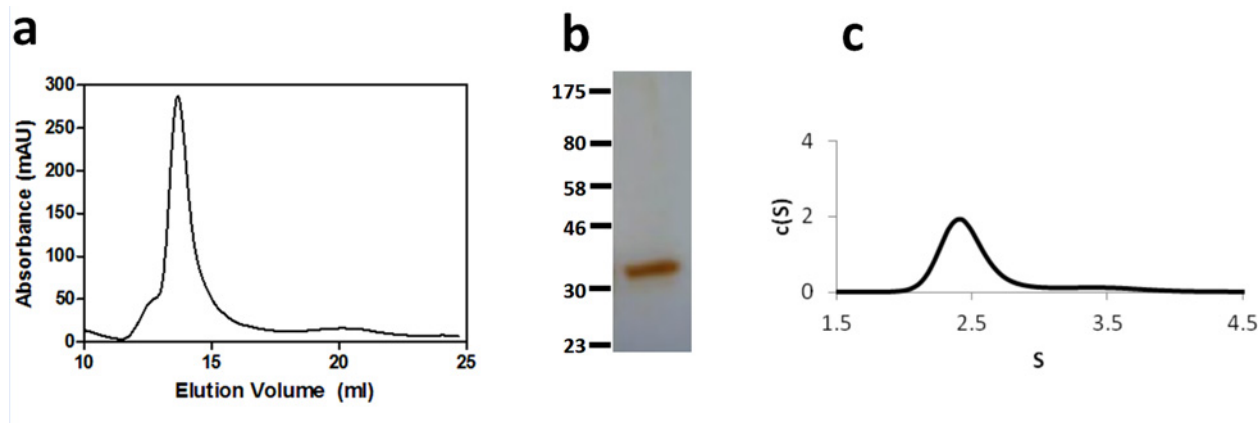
The vast majority of membrane proteins stabilized in nanodiscs to-date have used the MSP-based system developed by

Figure 2 Thermostability of A$_{2A}$R–SMALP and DDM-solubilized A$_{2A}$R from *P. pastoris*
A$_{2A}$R–SMALP (●) and DDM-solubilized A$_{2A}$R (▲) prepared from *P. pastoris* overexpressing A$_{2A}$R were incubated for 30 min at the stated temperatures, chilled on ice, before specific binding of [^{3}H]ZM241385 was determined as described in 'Methods'. Data are expressed as specific binding relative to the 20 °C data point (mean ± S.E.M. of three separate experiments performed in triplicate).

Sligar and colleagues [12]. In this MSP method, the lipid disc is stabilized by an annulus of scaffolding proteins which can interfere with spectrophotometric studies on the embedded membrane protein of interest. In contrast, the lipid disc in our SMALP system is stabilized by a non-proteinacious polymer, which we have already shown in a previous study, does not suffer from the same limitations [15]. This allowed the conformation of the SMALP-encapsulated A$_{2A}$R to be studied using CD spectroscopy. It is known from solved crystal structures that the A$_{2A}$R possesses a high α-helix content due to the seven transmembrane helical bundle that is a conserved feature of GPCR architecture [31,32]. The far-UV (195–260 nm) CD spectrum of purified A$_{2A}$R–SMALP showed negative minima at 208 and 222 nm consistent with a folded protein containing a high degree of α-helix (Figure 4), consistent with the known secondary structure content of the A$_{2A}$R. In contrast, an unfolded protein would have a

Figure 3   Analysis of A$_{2A}$R–SMALP from *P. pastoris* by size-exclusion chromatography and AUC
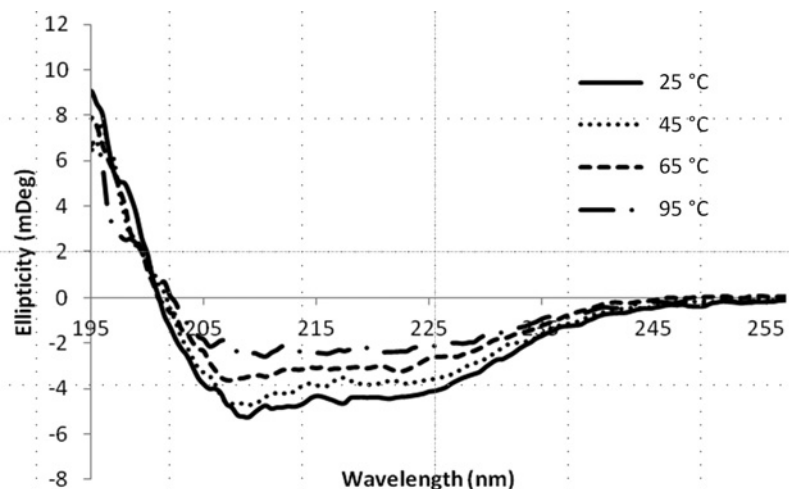(**a**) elution profile of A$_{2A}$R–SMALP from a Superdex 200 10/300GL size exclusion column with absorbance measured at 280 nm. (**b**) silver stained SDS/PAGE of the main peak eluted from the size exclusion chromatography. (**c**) plot of c(S) compared with sedimentation coefficient for A$_{2A}$R–SMALP.

negative minimum at 200 nm. CD was also used to assess the thermal stability of the encapsulated A$_{2A}$R. These data show that as the temperature increases from 25 °C to 95 °C the intensity of the 208 and 222 nm features reduces until at 95 °C the intensity is less than 50 % of that observed at low temperature. This indicates that the protein is steadily losing secondary structure as the temperature increases. Closer examination of the CD spectra shows a single isodichroic point at ∼201 nm. This indicates that the thermal denaturation process is a two state process most probably correlating with a folded to unfolded transition. Comparison of the CD spectra in Figure 4 to the thermostability binding data (Figure 2) revealed that the change in the CD spectrum observed between 25 °C and 65 °C reflected the structural changes underlying the complete loss of [^{3}H]ZM241385 binding by the A$_{2A}$R. The A$_{2A}$R was not fully denatured when the radioligand-binding capability was lost; however, as α-helix content was still apparent in the CD spectrum at 65 °C. The proportion of α-helix decreased further as the temperature was raised from 65 °C to 95 °C but even at 95 °C the A$_{2A}$R CD signal had not completely changed to that of a random coil (characterized by an intense negative signal at 200 nm and a positive signal at 218 nm [33]). This indicates that the helical secondary structure of the A$_{2A}$R is resistant to thermal denaturation in SMALPs. Retention of α-helical content has also been reported for rhodopsin during denaturation studies with combinations of different denaturants. Furthermore, it was concluded that surface elements within the rhodopsin structure were susceptible to denaturation, becoming more flexible [34], whereas a cluster of interconnected segments from multiple transmembrane helices preserved a rigid core [35]. This could explain our observations on the effect of increasing temperature on the A$_{2A}$R structure and function. Molecular dynamics simulations indicate that the process of a ligand binding to its cognate GPCR progresses through an intermediate state in which the ligand binds initially to an extracellular vestibule prior to docking in the classical 'orthosteric'-binding site [36,37]. The rhodopsin un-

folding studies cited above indicate that surface elements within the A$_{2A}$R architecture would be more susceptible to structural perturbation than the relatively rigid α-helical core. This suggests a feasible mechanism for our observations that the ligand-binding capability of the A$_{2A}$R was lost at temperatures which preserved significant α-helical content, albeit lower than native A$_{2A}$R. If the conformations of extracellular structural elements that contribute to the approach of a ligand to the orthosteric-binding site via the extracellular vestibule were susceptible to thermal disruption, then ligand binding capability would be ablated but core α-helical structure would be largely retained.

Characterization of A$_{2A}$R–SMALP from transfected HEK293T cells

The utility of SMALPs for purifying a functional human GPCR from *P. pastoris* for investigation by biophysical approaches has been demonstrated above. However, the exact lipid composition of the yeast plasma membrane is different from mammalian cells, most notably perhaps in lacking cholesterol and possessing ergosterol [38]. The nature of the lipids juxtaposed to a GPCR can affect the function. For example, cholesterol can modulate the activity of some GPCRs [39,40], can affect receptor conformation [41] and has been co-crystallized with GPCRs, which led to a 'cholesterol consensus motif' being proposed as part of a specific cholesterol-binding site within the architecture of some GPCRs [42]. As the SMALP-solubilization process involves the SMA polymer excising the receptor embedded in a nanodisc of native membrane bilayer [15] the lipid composition preserved in the A$_{2A}$R–SMALP is dictated by the composition of the cell membrane in which the receptor was expressed. There will be instances, such as drug discovery assays, when it will be desirable to preserve the more physiological annular lipid composition provided by a mammalian cell membrane. Consequently, we also characterized A$_{2A}$R–SMALP from transfected HEK293T cells.

Figure 4   The effect of temperature on $A_{2a}R$ structure revealed by CD spectra of purified $A_{2a}R$–SMALP
CD spectra were collected using a 1-mm path length cuvette and averaged over eight scans in the far-UV region (195–260 nm). Spectra were corrected for the buffer signal.
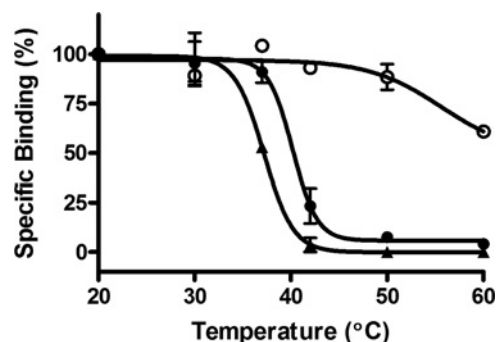
Table 2 Pharmacological characterization of $A_{2A}R$–SMALP from HEK293T cells
For each ligand, the pK_i value is presented for binding to $A_{2A}R$ in HEK293T membranes and also $A_{2A}R$–SMALP generated from the HEK293T cell membranes. Data are mean $\pm$ S.E.M. ($n = 3$).

Ligand	HEK membranes	HEK–SMALP
ZM241385	8.87 ± 0.1	8.53 ± 0.04
XAC	7.17 ± 0.19	6.38 ± 0.16
NECA	5.29 ± 0.1	5.39 ± 0.41
Theophylline	4.87 ± 0.12	4.97 ± 0.27

Figure 5 Thermostability of $A_{2a}R$–SMALP, DDM-solubilized $A_{2a}R$ and membrane-bound $A_{2a}R$ prepared from HEK293T cells
$A_{2a}R$–SMALP ($\bullet$), DDM-solubilized $A_{2a}R$ ($\blacktriangle$) or membranes ($\circ$), prepared from HEK293T cells transfected with $A_{2a}R$, were incubated for 30 min at the stated temperatures, then chilled on ice, before specific binding of [³H]ZM241385 was determined as described in 'Methods'. Data are expressed as specific binding relative to the 20°C data point (mean $\pm$ S.E.M. of three separate experiments performed in triplicate).

HEK293T cells, expressing $A_{2A}R$, were directly solubilized with 2.0% (w/v) SMA, in the total absence of detergent, to generate a functional $A_{2A}R$–SMALP preparation of 2.0 ± 0.24 pmol/mg protein ($n = 3$), equivalent to $23.3 \pm 2.75\%$ ($n = 3$) recovery of $A_{2A}R$. Characterization of this $A_{2A}R$–SMALP by competition radioligand-binding using a range of ligands with [³H]ZM241385 as tracer confirmed retention of typical $A_{2A}R$ pharmacology (Table 2). The $A_{2A}R$–SMALP from HEK293T cells exhibited an increase in thermostability of 4°C compared with the corresponding detergent (DDM)-solubilized $A_{2A}R$ (Figure 5), with the T_{50} value increasing from $T_{50} = 36.2 \pm 0.52$°C ($n = 3$) for $A_{2A}R$–DDM to $T_{50} = 40.2 \pm 0.44$°C ($n = 3$) for $A_{2A}R$–SMALP. The $A_{2A}R$–SMALP was not as stable as $A_{2A}R$ embedded in the native HEK293T cell membrane however (Figure 5).
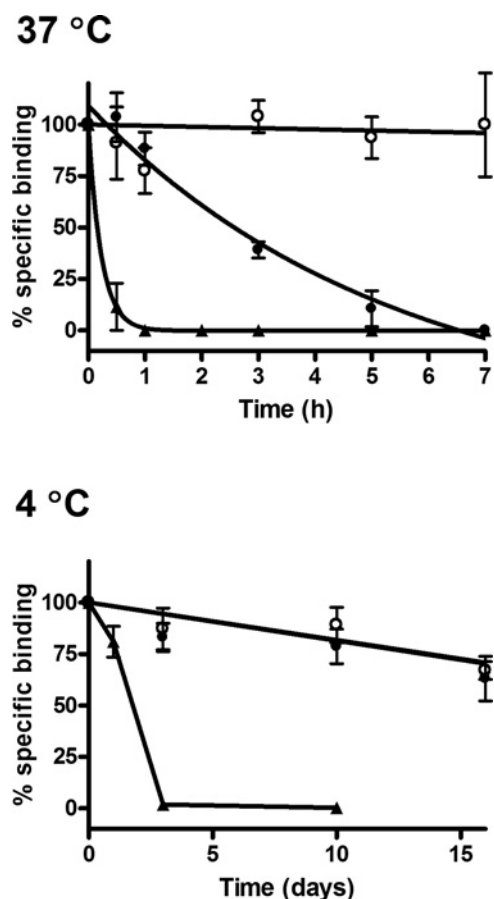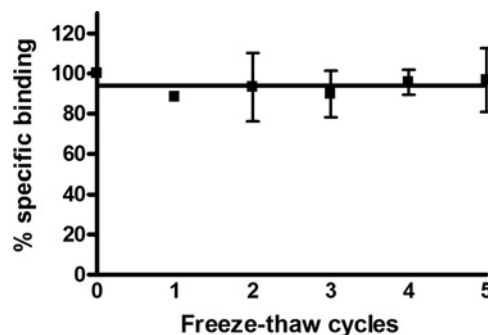
Given the potential utility of the GPCR–SMALP for receptor-based *in vitro* assays and screens, the stability of the $A_{2A}R$–SMALP at the physiological temperature of 37°C and the storage temperature of 4°C was investigated together with the resistance to repeated freeze-thaw cycles. A comparison of the loss of ligand binding capability of the $A_{2A}R$ at 37°C with time is presented in Figure 6 for $A_{2A}R$–DDM, $A_{2A}R$–SMALP and

cell membranes. The improved stability of the $A_{2A}R$–SMALP over $A_{2A}R$–DDM at 37°C is very marked, with a 7-fold increase in the half-life of [³H]ZM241385 binding ($A_{2A}R$–DDM, $t_{\frac{1}{2}} = 21 \pm 7$ min; $A_{2A}R$–SMALP, $t_{\frac{1}{2}} = 148 \pm 13$ min). This improvement is particularly apparent after 1 h, with no specific binding detected for the detergent-solubilized receptor, whereas $85 \pm 5\%$ of the binding was retained in the $A_{2A}R$–SMALP (Figure 6). Although receptor stability was increased in the SMALP, it did not match receptor stability in the native HEK293T membranes at 37°C, suggesting that not all the stabilizing factors of the plasma membrane are incorporated into SMALPs. In contrast, the stability of $A_{2A}R$–SMALP at 4°C was essentially

37 °C

4 °C

Figure 6 Comparison of A₂ₐR stability in different preparations at 37C and 4C

A$_{2a}$R–SMALP (●), DDM-solubilized A$_{2a}$R (▲) or membranes (○), prepared from HEK293T cells transfected with A$_{2a}$R, were incubated at 37 °C (top panel) or 4 °C (bottom panel), for the stated times. Specific binding of [³H]ZM241385 was determined at each time point. Data are expressed as specific binding relative to time zero (mean ± S.E.M. of three separate experiments performed in triplicate).

indistinguishable from that of membranes with $t_{\frac{1}{2}} \geqslant 16$ days, whereas A$_{2A}$R–DDM exhibited a $t_{\frac{1}{2}} = 1.8 \pm 0.3$ days (mean ± S.E.M.). The resilience of A$_{2A}$R–SMALP was also evident from repeated freeze/thaw cycles (Figure 7). Even after five freeze/thaw cycles on the same sample, there was no decrease in [³H]ZM241385 binding capability of the A$_{2A}$R–SMALP. In contrast, specific binding to the A$_{2A}$R–DDM preparation was completely lost after a single freeze-thaw cycle. Our data indicate that it is feasible to SMALP solubilize GPCRs and store them at 4 °C until required. Interestingly, the increase in thermostability endowed on A$_{2A}$R by the SMALP compared with DDM was approximately 5 °C for both yeast and HEK 293T, suggesting that the increased thermostability is an inherent property of the SMALP rather than due to differences in the lipid composition of the original membrane.

Figure 7 Effect of repeated freeze-thaw cycles on A₂ₐR–SMALP binding capability

A$_{2a}$R–SMALP was subjected to repeated freeze/thaw cycles and specific binding of [³H]ZM241385 determined after each cycle. Data are expressed as specific binding relative to binding before freezing (mean ± S.E.M. of three separate experiments performed in triplicate).

CONCLUSION

Strategies to ameliorate the detrimental effect of exposing GPCRs to detergents have included; modifying the detergent to reduce perturbation to the receptor [4], modifying the receptor to increase stability to detergent either by alanine scanning [43] or by molecular evolution [44] and simply reducing the detergent exposure time by inserting the detergent-solubilized receptor into nanodiscs stabilized by scaffolding proteins [9]. However, the ideal option would be to extract GPCR from the membrane, for purification or downstream assays, without the requirement for detergent. In the present study, we report the first purification of a GPCR (human A$_{2A}$R), without exposure to detergent at any stage, by exploiting spontaneous encapsulation direct from a membrane into a nanoscale SMALP. The A$_{2A}$R–SMALP, generated from both yeast and mammalian cells, exhibited increased thermostability compared with DDM-solubilized receptor that will facilitate use in receptor-based assays/screens. Furthermore, in contrast with nanodiscs stabilized by scaffold proteins, the non-proteinaceous nature of the SMA polymer does not interfere with biophysical characterization of the embedded receptor.

REFERENCES

1 Wheatley, M., Wootten, D., Conner, M.T., Simms, J., Kendrick, R., Logan, R.T., Poyner, D.R. and Barwell, J. (2012) Lifting the lid on G-protein-coupled receptors: the role of extracellular loops. Brit. J. Pharmacol. **165**, 1688–1703 CrossRef

2 Lagerström, M.C. and Schiöth, H.B. (2008) Structural diversity of G-protein-coupled receptors and significance for drug discovery. Nat. Rev. Drug Discov. **7**, 339–357 CrossRef PubMed

3 Popot, J.-L. (2010) Amphipols, nanodiscs and fluorinated surfactants: three nonconventional approaches to studying membrane proteins in aqueous solutions. Annu. Rev. Biochem. **79**, 737–775 CrossRef PubMed

4 Chae, P.S., Rasmussen, S.G., Rana, R.R., Gotfryd, K., Chandra, R., Goren, M.A., Kruse, A.C., Nurva, S., Loland, C.J., Pierre, Y. et al. (2010) Maltose-neopentyl glycol (MNG) amphiphiles for solubilization, stabilization and crystallization of membrane proteins. Nat. Methods **7**, 1003–1008 CrossRef PubMed

5 Banères, J.L., Popot, J.L. and Mouillac, B. (2011) New advances in production and functional folding of G-protein-coupled receptors. Trends Biotechnol. **29**, 314–322 CrossRef PubMed

6 Nehmé, R., Joubert, O., Bidet, M., Lacombe, B., Polidori, A., Pucci, B. and Mus-Veteau, I. (2010) Stability study of the human G-protein-coupled receptor, smoothened. Biochim. Biophys. Acta **1798**, 1100–1110 CrossRef PubMed

7 Tao, H., Lee, S.C., Moeller, A., Roy, R.S., Siu, F.Y., Zimmermann, J., Stevens, R.C., Potter, C.S., Carragher, B. and Zhang, Q. (2013) Engineered nanostructured β-sheet peptides protect membrane proteins. Nat. Methods **10**, 759–761 CrossRef PubMed

8 Bayburt, T.H., Grinkova, Y.V. and Sligar, S.G. (2002) Self-assembly of discoidal phospholipid bilayer nanoparticles with membrane scaffold proteins. Nano Lett. **2**, 853–856 CrossRef

9 Leitz, A.J., Bayburt, T.H., Barnakov, A.N., Springer, B.A. and Sligar, S.G. (2006) Functional reconstitution of β_2-adrenergic receptors utilizing self-assembling nanodisc technology. Biotechniques **40**, 601–610 CrossRef PubMed

10 Whorton, M.R., Bokoch, M.P., Rasmussen, S.G., Huang, B., Zare, R.N., Kobilka, B. and Sunahara, R.K. (2007) A monomeric G protein-coupled receptor isolated in a high-density lipoprotein particle efficiently activates its G protein. Proc. Natl. Acad. Sci. U.S.A. **104**, 7682–7687 CrossRef PubMed

11 Banerjee, S., Huber, T. and Sakmar, T.P. (2008) Rapid incorporation of functional rhodopsin into nanoscale apolipoprotein-bound bilayer (NABB) particles. J. Mol. Biol. **377**, 1067–1081 CrossRef PubMed

12 Denisov, I.G., Grinkova, Y.V., Lazarides, A.A. and Sligar, S.G. (2004) Directed self-assembly of monodisperse phospholipid bilayer nanodiscs with controlled size. J. Am. Chem. Soc. **126**, 3477–3487 CrossRef PubMed

13 Nath, A., Atkins, W.M. and Sligar, S.G. (2007) Applications of phospholipid bilayer nanodiscs in the study of membranes and membrane proteins. Biochemistry **46**, 2059–2069 CrossRef PubMed

14 Mitra, N., Liu, Y., Liu, J., Serebryany, E., Mooney, V., DeVree, B.T., Sunahara, R.K. and Yan, E.C.Y. (2013) Calcium-dependent ligand binding and G-protein signalling of family B parathyroid hormone 1 receptor purified in nanodiscs. ACS Chem. Biol. **8**, 617–625 CrossRef PubMed

15 Knowles, T.J., Finka, R., Smith, C., Lin, Y.-P., Dafforn, T. and Overduin, M. (2009) Membrane proteins solubilized intact in lipid containing nanoparticles bounded by styrene maleic acid copolymer. J. Am. Chem. Soc. **131**, 7484–7485 CrossRef PubMed

16 Jamshad, M., Rajesh, S., Stamataki, Z., McKeating, J.A., Dafforn, T., Overduin, M. and Bill, R.M. (2008) Structural characterization of recombinant human CD81 produced in *Pichia pastoris*. Protein Expr. Purif. **57**, 206–217 CrossRef PubMed

17 Singh, S., Gras, A., Fiez-Vandal, C., Ruprecht, J., Rana, R., Martinez, M., Strange, P.G., Wagner, R. and Byrne, B. (2008) Large-scale functional expression of WT and truncated human adenosine A_{2A} receptor in *Pichia pastoris* bioreactor cultures. Microb. Cell Fact. **7**, 28 CrossRef PubMed

18 Fraser, N.J. (2006) Expression and functional purification of a glycosylation deficient version of the human adenosine 2a receptor for structural studies. Protein Expr. Purif. **49**, 129–137 CrossRef PubMed

19 Conner, A.C., Simms, J., Howitt, S.G., Wheatley, M. and Poyner, D.R. (2006) The second intracellular loop of the CGRP-receptor provides molecular determinants for signal transduction and cell surface expression. J. Biol. Chem. **281**, 1644–1651 CrossRef PubMed

20 Wheatley, M., Howl, J., Yarwood, N.J., Davies, A.R.L. and Parslow, R.A. (1997) Preparation of a membrane fraction for receptor studies and solubilization of receptor proteins with retention of biological activity. Methods Mol. Biol. **73**, 305–332 PubMed

21 Cheng, Y. and Prusoff, W.H. (1973) Relationship between the inhibition constant (K_i) and the concentration of inhibitor which causes 50 per cent inhibition (IC_{50}) of an enzymatic reaction. Biochem. Pharmacol. **22**, 3099–3108 CrossRef PubMed

22 Schuck, P. (2000) Size-distribution analysis of macromolecules by sedimentation velocity ultracentrifugation and lamm equation modeling. Biophys. J. **78**, 1606–1619 CrossRef PubMed

23 Laue, T.M., Shah, B.D., Ridgeway, T.M. and Pelletier, S.L. (1992) Computer-aided interpretation of analytical sedimentation data for proteins. In Analytical Ultracentrifugation in Biochemistry and Polymer Science (Harding, S.E., Rowe, A.J. and Horton, J.C., eds), pp. 90–125, Royal Society of Chemistry, London

24 Hino, T., Arakawa, T., Iwanari, H., Yurugi-Kobayashi, T., Ikeda-Suno, C., Nakada-Nakura, Y., Kusano-Arai, O., Weyand, S., Shimamura, T., Nomura, N. et al. (2012) G-protein-coupled receptor inactivation by an allosteric inverse-agonist antibody. Nature **482**, 237–240 PubMed

25 Shimamura, T., Shiroishi, M., Weyand, S., Tsujimoto, H., Winter, G., Katritch, V., Abagyan, R., Cherezov, V., Liu, W., Han, G.W. et al. (2011) Structure of the histamine H1 receptor complex with doxepin. Nature **475**, 65–70 CrossRef PubMed

26 Bonander, N., Darby, R.A., Grgic, L., Bora, N., Wen, J., Brogna, S., Poyner, D.R., O'Neill, M.A. and Bill, R.M. (2009) Altering the ribosome subunit ratio in yeast maximizes recombinant protein yield. Microb. Cell Fact. **8**, 10 CrossRef PubMed

27 Jamshad, M., Lin, Y.-P., Knowles, T.J., Parslow, R.M., Harris, C., Wheatley, M., Poyner, D.R., Bill, R.M., Thomas, O.R.T., Overduin, M. and Dafforn, T.R. (2011) Surfactant-free purification of membrane proteins with intact native membrane environment. Biochem. Soc. Trans. **39**, 813–818 PubMed

28 Miller, D., Charalambous, K., Rotem, D., Schuldiner, S., Curnow, P. and Booth, P. (2009) *In vitro* unfolding and refolding of the small multidrug transporter EmrE. J. Mol. Biol. **393**, 815–832 CrossRef PubMed

29 Orwick-Rydmark, M., Lovett, J.E., Graziadei, A., Linholm, L., Hicks, M.R. and Watts, A. (2012) Detergent-free incorporation of a seven-transmembrane receptor protein into nanosized bilayer lipodisq particles for functional and biophysical studies. Nano Lett. **12**, 4687–4692 CrossRef PubMed

30 Gulati, S., Jamshad, M., Knowles, T.J., Morrison, K.A., Downing, R., Cant, N., Collins, R., Koenderink, J.B., Ford, R.C., Overduin, M. et al. (2014) Detergent-free purification of ABC transporters. Biochem. J. **461**, 269–278 CrossRef PubMed

31 Jaakola, V.-P., Griffith, M.T., Hanson, M.A., Cherezov, V., Chien, E.Y.T., Lane, J.R., Ijzerman, A.P. and Stevens, R.C. (2008) The 2.6 angstrom crystal structure of a human A_{2A} adenosine receptor bound to an antagonist. Science **322**, 1211–1217 CrossRef PubMed

32 Lebon, G., Warne, T., Edwards, P.C., Bennett, K., Langmead, C.J., Leslie, A.G.W. and Tate, C.G. (2011) Agonist-bound adenosine A_{2A} receptor structures reveal a common features of GPCR activation. Nature **474**, 521–525 CrossRef PubMed

33 Rodger, A., Dafforn, T. and Norden, B. (2010) Linear Dichroism and Circular Dichroism Royal Society of Chemistry, Cambridge

34 Dutta, A., Kim, T.-Y., Moeller, M., Wu, J., Alexiev, U. and Klein-Seetharaman, J. (2010) Characterization of membrane protein non-native states. 2. The SDS-unfolded states of rhodopsin. Biochemistry **49**, 6329–6340 CrossRef PubMed

35 Tastan, O., Dutta, A., Booth, P. and Klein-Seetharaman, J. (2014) Retinal proteins as model systems for membrane protein folding. Biochim. Biophys. Acta **1837**, 656–663 CrossRef PubMed

36 Dror, R.O., Pan, A.C., Arlow, D.H., Borhani, D.W., Maragakis, P., Shan, Y., Xu, H. and Shaw, D.E. (2011) Pathway and mechanism of drug binding to G-protein-coupled receptors. Proc. Natl. Acad. Sci. U.S.A. **108**, 13118–13123 CrossRef PubMed

37 Dror, R.O., Green, H.F., Valant, C., Borhani, D.W., Valcourt, J.R., Pan, A.C., Arlow, D.H., Canals, M., Lane, J.R., Rahmani, R. et al. (2013) Structural basis for modulation of a G-protein-coupled receptor by allosteric drugs. Nature **503**, 295–299 PubMed

38 Finean, J.B., Coleman, R. and Michell, R.H. (1978) Membranes and Their Cellular Functions, 2nd edn, Blackwell Scientific Publications, Oxford

39 Gimpl, G., Burger, K. and Fahrenholz, F. (1997) Cholesterol as modulator of receptor function. Biochemistry **36**, 10959–10974 CrossRef PubMed

40 Pang, L., Graziano, M. and Wang, S. (1999) Membrane cholesterol modulates galanin-GalR2 interaction. Biochemistry **38**, 12003–12011 CrossRef PubMed

41 Muth, S., Fries, A. and Gimpl, G. (2011) Cholesterol-induced conformational changes in the oxytocin receptor. Biochem. J. **437**, 541–553 CrossRef PubMed

42 Hanson, M.A., Cherezov, V., Griffith, M.T., Roth, C.B., Jaakola, V.P., Chien, E.Y., Velasquez, J., Kuhn, P. and Stevens, R.C. (2008) A specific cholesterol binding site is established by the 2.8Å structure of the human β2-adrenergic receptor. Structure **16**, 897–905 CrossRef PubMed

43 Serrano-Vega, M.J., Magnani, F., Shibata, Y. and Tate, C.G. (2008) Conformational thermostabilization of the beta1-adrenergic receptor in a detergent-resistant form. Proc. Natl. Acad. Sci. U.S.A. **105**, 877–882 CrossRef PubMed

44 Scott, D.J. and Plückthun, A. (2013) Direct molecular evolution of detergent-stable G-protein-coupled receptors using polymer encapsulated cells. J. Mol. Biol. **425**, 662–677 CrossRef PubMed